

# Demonstration of distributed shape sensing based on Brillouin scattering in multi-core fibers

Zhiyong Zhao<sup>a,b</sup>, Marcelo A. Soto<sup>a</sup>, Ming Tang<sup>b,\*</sup>, Luc Thévenaz<sup>a,\*</sup>

<sup>a</sup>EPFL Swiss Federal Institute of Technology, Institute of Electrical Engineering, SCI STI LT, Station 11, CH-1015 Lausanne, Switzerland

<sup>b</sup>National Engineering Laboratory for Next Generation Internet Access System, School of Optics and Electronic Information, Huazhong University of Science and Technology, Wuhan 430074, China

\*Corresponding author: tangming@mail.hust.edu.cn; luc.thevenaz@epfl.ch

## ABSTRACT

In this paper we demonstrate distributed shape sensing based on stimulated Brillouin scattering in a multi-core fiber (MCF). Brillouin optical time-domain analysis with differential pulse-width pairs is implemented to measure the local tangential strain-induced variation of the Brillouin frequency shift along different cores of the fiber. Employing the differential strain measured in multiple off-center cores in the MCF, distributed profiles of both bending angle and fiber curvature are parametrically retrieved. The paper presents the first demonstration of distributed bending sensing, providing the cornerstone to further develop the system into a fully distributed 3D shape sensor.

**Keywords:** Multi-core fiber, Brillouin scattering, distributed fiber sensor, bending sensor, shape sensing

## INTRODUCTION

As one of the most promising distributed optical fiber sensing technique, Brillouin distributed sensing has been mainly dedicated to the measurement of temperature and strain over the last two decades, with intensive efforts made to enhance the system's performance in terms of sensing length and spatial resolution<sup>1</sup>. The technique is mainly implemented in single-mode fibers (SMFs). In recent years, Brillouin distributed sensors employing special fibers, e.g. photonic crystal fibers<sup>2</sup>, polymer optical fibers<sup>3</sup>, few mode fibers<sup>4</sup>, have also been reported. However most of the work in this prior literature has only demonstrated the ability to measure the conventional parameters, i.e. temperature and/or strain.

On the other hand, driven by the increasing transmission capacity demand, space division multiplexing (SDM) technique using multi-core fibers have shown great feasibility and superiority for optical fiber communication. In fact, the unique feature of MCF, containing multiple spatially isolated and independently transmitted channels, also provides a platform for distributed sensing applications. Recently, we reported the observation of the bending-dependence of the Brillouin frequency shift (BFS) in off-center cores in a MCF<sup>5</sup>, revealing that the BFS varies with a linear dependence on the local fiber curvature (the reciprocal of bending radius). This has demonstrated the potential of MCFs for distributed curvature and shape sensing based on conventional Brillouin sensing interrogation techniques.

In this paper, we demonstrate distributed curvature and shape sensing based on Brillouin optical time-domain analysis (BOTDA) measurements in a MCF. In particular, distributed BFS profiles in multiple off-center cores are measured with sub-metric resolution using differential pulse-width pairs (DPP-) BOTDA<sup>6</sup>. The differential strain in the different cores is determined based on the linear dependence of the BFS on the fiber curvature. A parametric calculation is then used to retrieve the local bending angle and curvature along the MCF. The theoretical description and experimental results show how conventional BFS measurements in MCF can be exploited to reconstruct the distributed profile of the fiber shape with high efficiency, noting that no additional process (e.g. inscribing a fiber Bragg grating) is required on the sensing fiber. Results strongly support the approach of using standard Brillouin sensing methods in MCFs to measure new physical quantities, thus establishing a new avenue towards diversified fiber sensing approaches.

## WORKING PRINCIPLE

The principle of the here proposed method for distributed shape sensing is based on the linear dependence that the BFS of off-center cores in MCFs shows on the fiber curvature<sup>5</sup>. In particular, when a MCF is bent at a given position,

different tangential strains are locally induced in each of the lateral cores, thus leading to different variations of the BFS. For the  $i$ -th core, this bending-induced BFS change can be written as:

$$\Delta v_{Bi} = \alpha \cdot v_B \cdot \varepsilon_i \quad (1)$$

where  $\Delta v_{Bi}$  is the variation of BFS of core  $i$ ,  $\alpha$  is the curvature-induced strain response coefficient,  $v_B$  is the initial BFS in a straight fiber section without strain,  $\varepsilon_i$  is the locally-induced strain in core  $i$ , which is determined by the fiber geometric parameters and bending angle, as

$$\varepsilon_i = -\frac{d_i}{R} \cos(\theta_b - \theta_i) \quad (2)$$

where  $d_i$  is the distance of core  $i$  to the center of the fiber,  $R$  is the bending radius,  $\theta_b$  and  $\theta_i$  are respectively the bending angle and the angular position of core  $i$ , where  $\theta_b$  is defined to be the angular offset from the local  $x$ -axis to the local fiber bending direction, and  $\theta_i$  is the angle from local  $x$ -axis to core  $i$ , as shown in Fig. 1(a). Note that the value of  $\alpha$  is the same as the one reported in Ref. 5 (i.e.  $\alpha = -4.883$ ), since the same MCF is used here for experiment.

The measurement of BFS in every individual core of the MCF can be used to obtain the local strain that the core experiences, as indicated by Eq. (1). Then, as described in Eq. (2), for a specific core in the MCF, its local strain can be used to determine the local bending radius and bending angle. Actually the differential strain profiles in the different cores provide relevant information to retrieve the bending angle and bending radius of the sensing fiber. For this, an apparent curvature vector  $K_i$  is defined for each core  $i$ . The magnitude of this vector depends on the induced strain and the radial distance between the core and the fiber center, while its direction depends on the angular offset of the core<sup>7</sup>. Using  $N$  cores, the vector sum  $K$  of the apparent curvature vectors  $K_i$  is defined as:

$$K(z) = -\sum_{i=1}^N \frac{\varepsilon_i(z)}{d_i} \cos \theta_i \hat{i} - \sum_{i=1}^N \frac{\varepsilon_i(z)}{d_i} \sin \theta_i \hat{j} \quad (3)$$

where  $\hat{i}$  and  $\hat{j}$  are unit vectors aligned with the local  $x$ - and  $y$ -axis, respectively. From Eq. (3) the local bending angle  $\theta_b(z)$  and curvature  $\kappa(z)$  (the reciprocal of bending radius) can be calculated as<sup>5,7</sup>:

$$\theta_b(z) = \cos^{-1} \left( \frac{K_x(z)}{|K(z)|} \right) = \sin^{-1} \left( \frac{K_y(z)}{|K(z)|} \right) = \tan^{-1} \left( \frac{K_y(z)}{K_x(z)} \right) \quad (4)$$

$$\kappa(z) = \frac{|K(z)|}{\sqrt{\left( \sum_{i=1}^N \cos(\theta_b - \theta_i) \cos(\theta_i) \right)^2 + \left( \sum_{i=1}^N \cos(\theta_b - \theta_i) \sin(\theta_i) \right)^2}} \quad (5)$$

## EXPERIMENTAL SETUP, RESULTS AND DISCUSSION

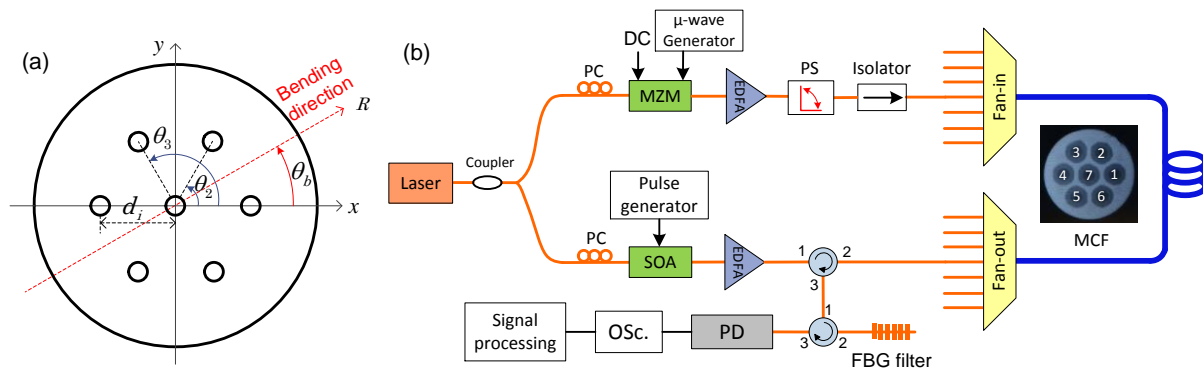


Figure 1 (a) the geometrical distribution of the 7-core fiber; (b) Experimental setup. PC: polarization controller; MZM: Mach-Zehnder modulator; SOA: semiconductor optical amplifier; EDFA: erbium-doped fiber amplifier; PS: polarization switch; FBG: fiber Bragg grating; PD: photodetector. OSC.: oscilloscope.

The experiment setup shown in Fig. 1(b) has been used to demonstrate distributed shape sensing based on conventional BOTDA, where the differential pulse-width pairs technique has been employed to achieve 20 cm spatial resolution<sup>6</sup>. The ~1 km-long MCF used in our experiment is a seven-core fiber, whose six outer cores are hexagonally arranged, as shown in the inset of Fig. 1(b). The nominal cladding diameter of the MCF is 150  $\mu\text{m}$  and the core pitch is ~40  $\mu\text{m}$ , respectively. The MCF is connected to the system through fan-in/out spatial Mux/De-Mux couplers at its two ends. To assess the effectiveness of the proposed method, different fiber shape profiles have been patterned close to the far end of the ~1 km-long MCF, as shown in Fig. 2, including four U-like profiles and three O-like profiles. It should be pointed out that, to provide a known reference of the bending angle for measurements to be compared with, the core's orientation of the patterned MCF has been positioned before measurement using the visual procedure as described in Ref. 5.

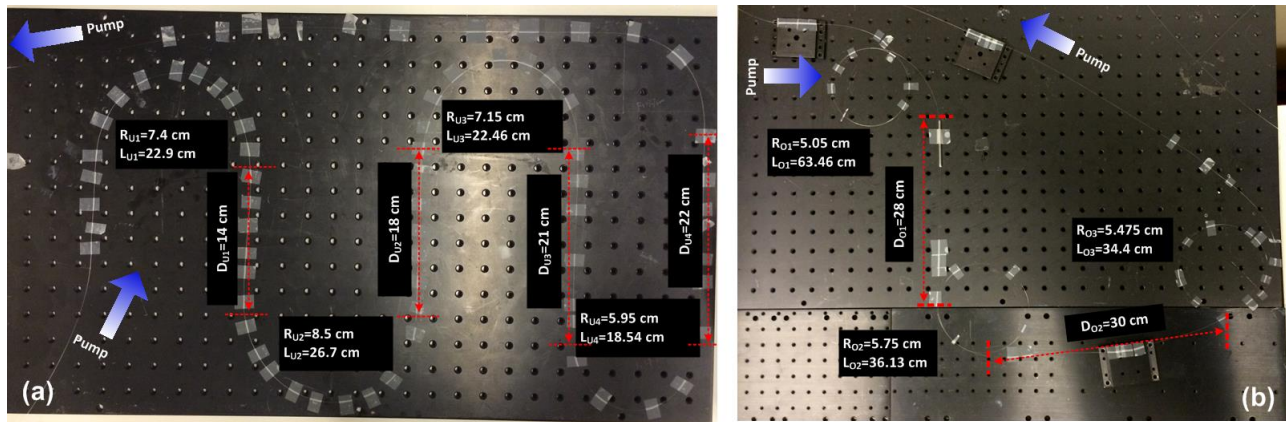


Figure 2. Shapes made for validating the ability of distributed shape sensing; (a) Four U-shapes, and (b) three O-shapes.

The BFS profiles measured along Core 1, Core 2 and Core 3 (see Fig. 1(a) and inset of Fig. 1(b)) are shown in Fig. 3, where the U-shape and O-shape regions can be easily identified in Fig. 3(a) and (b), respectively.

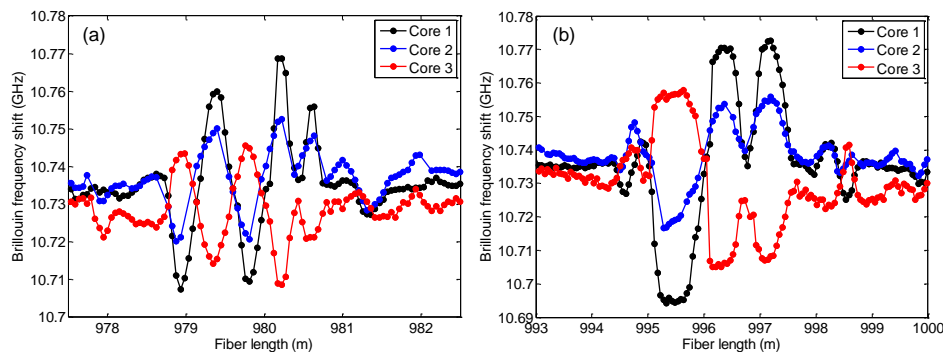


Figure 3. BFS profiles versus distance, measured along three cores at (a) the 4 U-shape regions and (b) the 3 O-shape regions.

Calculations have been conducted by using the acquired BFS profiles in order to retrieve the bending angles and bending radius of the seven patterns. The measured variation of BFS has been first converted into strain using Eq. (1) with the sensitivity value  $\alpha = -4.883$  obtained during prior characterization. The applied bending angle  $\theta_b(z)$  and curvature  $\kappa(z)$  of each pattern are then obtained solving Eqs. (3)-(5). Figures 4(a) and 4(b) show the retrieved bending angles of the 4 U-profiles and 3 O-profiles, while Figs. 4(c) and 4(d) show the curvature retrieved along the fiber. O-shapes have been labelled as “1” to “4” and U-shapes have been labelled as “5” to “7”. The propagation of the error (measurement noise) in the variables used in Eqs. (4)-(5) to calculate the bending angle and curvature has been evaluated and also shown in Fig. 4(a) and 4(b). Experimental results reveal that the uncertainties are in general quite low, but increase at locations where the bending angle changes very fast. This is believed to be caused by the large levels of torsion and a presumably insufficient spatial resolution to measure fast torsion changes. However, within the fiber sections having a uniform bending angle, for example within the calibrated shape regions, the standard deviation of the calculated bending angle and curvature is very small (less than 4.53 degree). The standard deviation is actually less than 1.63 degree for all three O-shapes; this better accuracy may be due to longer bending lengths used for these 3 O-shapes, which provide

more reliable and stable measurements. On the other hand, the comparison between retrieved and set bending radius (shown in Fig. 2(b)) reveals that the relative error in the radius  $R$  is below 8% in all cases. Results demonstrate the high accuracy and good reliability of the method for distributed shape sensing.

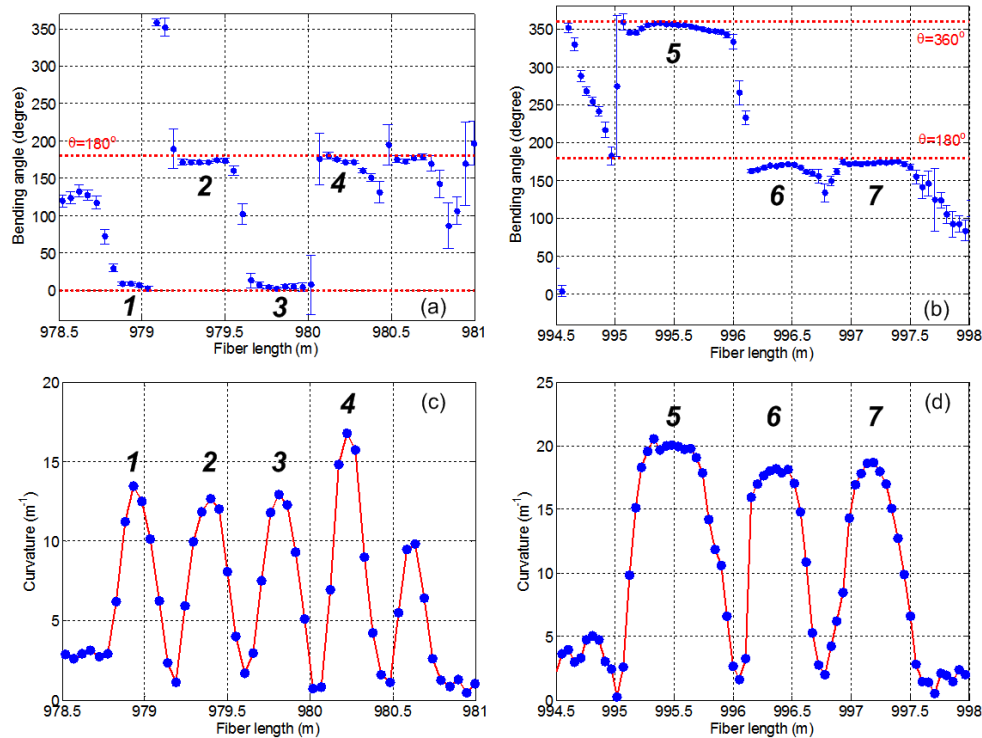


Figure 4. Retrieved bending angle for (a) the 4 U-shape region; (b) the 3 O-shape region, and curvature for (c) the 4 U-shape region and (d) the 3 O-shape region. Number “1” to “7” denotes the seven measured shapes.

In conclusion, a thorough experimental investigation on distributed curvature/shape sensing using Brillouin scattering in MCF has been presented and experimentally demonstrated. The measured distributed profiles of curvature and bending angle along the fiber give the basis to extend the technique to perform full 3D shape determination by solving the Frenet-Serret formulas<sup>7</sup>. The proposed scheme is much more efficient and simpler compared to the use of fiber Bragg gratings since the sensing fiber does not require any special preparation during or after fabrication; in addition it provides a fully distributed technique, which can provide much longer sensing ranges and no dead zones.

The authors thank Huifeng Wei and Weijun Tong from YOFC, China for providing the MCF, and EPFL-CIME for characterizing the geometry of the MCF. Z. Zhao acknowledges the China Scholarship Council and Andrey Denisov.

## REFERENCES

- [1] Motil, A., Bergman, A., and Tur, M., “State of the art of Brillouin fiber-optic distributed sensing,” *Optics & Laser Technology* 78(A), 81–103 (2016).
- [2] Zou, L., Bao, X., Afshar, S., and Chen, L., “Dependence of the Brillouin frequency shift on strain and temperature in a photonic crystal fiber,” *Opt. Lett.* 29(13), 1485–1487 (2004).
- [3] Mizuno, Y., and Nakamura, K., “Potential of Brillouin scattering in polymer optical fiber for strain-insensitive high-accuracy temperature sensing,” *Opt. Lett.* 35(23), 3985–3987 (2010).
- [4] Song, K.-Y., and Kim, Y.-H., “Characterization of stimulated Brillouin scattering in a few-mode fiber,” *Opt. Lett.* 38(22), 4841–4844 (2013).
- [5] Zhao, Z., Soto, M. A., Tang, M., and Thévenaz, L., “Curvature and shape distributed sensing using Brillouin scattering in multi-core fibers,” in *Advanced Photonics 2016*, paper SeM4D.4.
- [6] Li, W., Bao, X., Li, Y., and Chen, L., “Differential pulse-width pair BOTDA for high spatial resolution sensing,” *Opt. Express* 16(26), 21616–21625 (2008).
- [7] Moore, J. P., and Rogge, M. D., “Shape sensing using multi-core fiber optic cable and parametric curve solutions,” *Opt. Express* 20(3), 2967–2973 (2012).